Synthesis and crystallographic studies of garnet-type AgCa2Mn2V3O12 and NaPb2Mn2V3O12

Synthesis and Crystallographic Studies of Garnet-type $AgCa_2Mn_2V_3O_{12}$ and $NaPb_2Mn_2V_3O_{12}$

Junji Awaka[a,*,1], Norihito Kijima[a], Junji Akimoto[a], Shoichi Nagata[b]

[a]*National Institute of Advanced Industrial Science and Technology (AIST), Tsukuba Central 5, 1-1-1 Higashi, Tsukuba, Ibaraki 305-8565, Japan*

[b]*Department of Materials Science and Engineering, Muroran Institute of Technology, 27-1 Mizumoto-cho, Muroran, Hokkaido 050-8585, Japan*

Abstract

High-purity powder specimens of $AgCa_2Mn_2V_3O_{12}$ and $NaPb_2Mn_2V_3O_{12}$ have been successfully synthesized by solid-state chemical reaction. The Rietveld refinements from X-ray powder diffraction data verified that these compounds have the garnet-type structure (space group *Ia*-3*d*, No. 230) with the lattice constant of a = 12.596(2) Å for $AgCa_2Mn_2V_3O_{12}$ and a = 12.876(2) Å for $NaPb_2Mn_2V_3O_{12}$. Calculation of the bond valence sum supported that Mn is divalent and V is pentavalent in these garnets. Estimation of the quadratic elongation and the bond angle variance showed that the distortions of the MnO_6 octahedra and the VO_4 tetrahedra are significantly suppressed. Our new results of $AgCa_2Mn_2V_3O_{12}$ and $NaPb_2Mn_2V_3O_{12}$ are compared to those of $AgCa_2M_2V_3O_{12}$ and $NaPb_2M_2V_3O_{12}$ (M = Mg, Co, Ni, Zn).

Keywords: Inorganic compounds; Oxides; Chemical synthesis; X-ray diffraction; Crystal structure

Corresponding author.
E-mail address: j.awaka@aist.go.jp (J. Awaka).
[1]Research Fellow of the Japan Society for the Promotion of Science

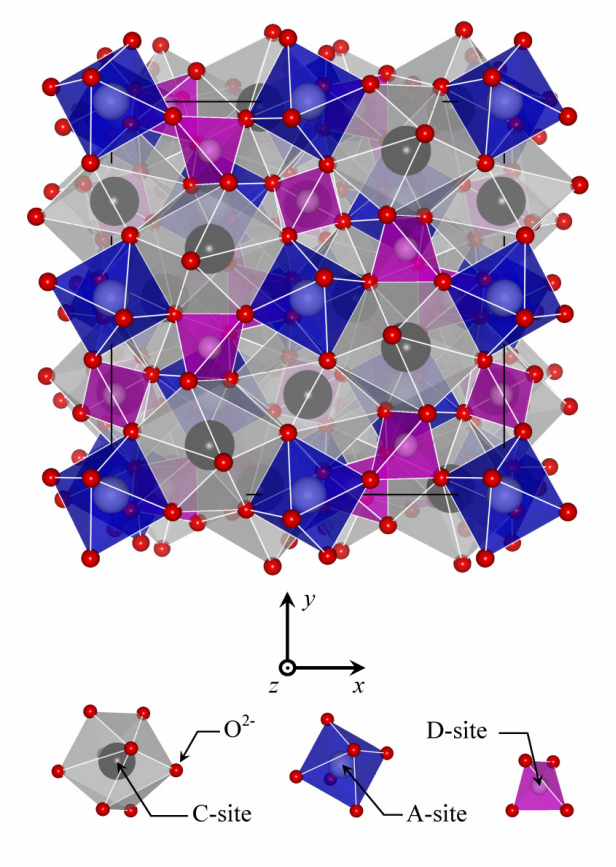

Fig. 1. Unit cell of garnet-type structure $\{C_3\}[A_2](D_3)O_{12}$ with space group *Ia*3-*d* (No. 230). The crystal structures were drawn with a computer program VICS [25].

1. Introduction

The garnet-type compounds have been attracting great interests on the magnetic properties in the theory and experiments [1-8], in particular, ferrimagnetism of rare-earth iron garnets $R_3Fe_5O_{12}$ (R = rare-earth element) [1-3].

The garnet structure has cubic symmetry of the space group *Ia*-3*d* (No. 230), as Fig. 1 depicts. The general structural formula for an oxide garnet can be represented as, $\{C_3\}[A_2](D_3)O_{12}$, with eight of these formula units per unit cell, where C-, A-, and D-sites are the cation sites. These cation sites are surrounded by oxygen ions O^{2-} at the vertices of a dodecahedron (C-site), octahedron (A-site), and tetrahedron (D-site), respectively. The structure is comprised of a three-dimensional framework by these polyhedrons sharing edges.

Generally, larger ions preferably occupy the larger sites, in the order of C-, A-, and D-sites. These cation sites are occupied by a wide variety of cations, for instance, alkali metal, alkaline earth metal, transition metal, and rare-earth ions can be appropriated by substituting either C- or A- or D-sites. A great number of garnet compounds with complex chemical compositions have been synthesized, in particular, non-iron garnet [1]. Oxide garnets with M ion at D-site are collectively dubbed 'M garnet', for instance, $\{AgCa_2\}[Mn_2](V_3)O_{12}$ and $\{NaPb_2\}[Mn_2](V_3)O_{12}$ so-called 'vanadium garnet'.

Table 1
Crystallographic data and details in the data collection and structure refinements

	$AgCa_2Mn_2V_3O_{12}$	$NaPb_2Mn_2V_3O_{12}$
Crystal system	cubic	cubic
Space group	*Ia*-3*d*	*Ia*-3*d*
Z	8	8
a (Å)	12.596(2)	12.876(2)
V (Å^3)	1998.3(4)	2134.6(8)
R_{wp} (%)	13.74	12.18
R_e (%)	10.37	9.13
R_p (%)	9.83	9.21
R_B (%)	4.67	3.75
R_F (%)	5.55	3.12
S	1.33	1.33
Wavelength (Å)	1.5418	1.5418
2θ range (°)	10 - 120	10 - 120
2θ step width (°)	0.02	0.02

Numbers in parentheses are the estimated standard deviations of the last significant digit.

Recently, we have successfully synthesized high-purity powder specimens of $AgCa_2Mn_2V_3O_{12}$ and $NaPb_2Mn_2V_3O_{12}$ by solid-state chemical reactions. In these compounds, Ag^+ and Ca^{2+} ions (or Na^+ and Pb^{2+} ions) occupy the C-sites, Mn^{2+} ions occupy the A-sites and V^{5+} ions occupy the D-sites. In the garnet structure, the body-centered-cubic sublattice is build by octahedral A-sites. Thus, $AgCa_2Mn_2V_3O_{12}$ and $NaPb_2Mn_2V_3O_{12}$ have only one magnetic sublattice of the A-site, therefore, which provides a much simpler magnetic interaction. Prior to the magnetic studies of $AgCa_2Mn_2V_3O_{12}$ and $NaPb_2Mn_2V_3O_{12}$, we here focus and report on the synthesis and crystallographic studies of these vanadium garnets.

Nearly 30 years ago, many works on the vanadium garnets were reported [9-18]. The vanadium garnets, $AgCa_2Mn_2V_3O_{12}$ and $NaPb_2Mn_2V_3O_{12}$, were synthesized for the first time by Ronniger et al. [9], where only the lattice constants were given. Subsequently, the structure analysis of single crystal of $AgCa_2Mn_2V_3O_{12}$ was carried out by Rettich [10]. No crystal structure investigation of $NaPb_2Mn_2V_3O_{12}$ has been reported yet, as far as we know.

In this work, the detailed structure analysis of $NaPb_2Mn_2V_3O_{12}$ has been made for the first time by the Rietveld refinement using X-ray powder diffraction (XRD) data. To compare with the structure analysis of single crystal of $AgCa_2Mn_2V_3O_{12}$ [10], the crystallographic study for this compound has been re-investigated by the Rietveld refinement. The present work is an extension of our previous studies of $AgCa_2M_2V_3O_{12}$ (M = Co, Ni, Cu, Zn) and $NaPb_2M_2V_3O_{12}$ (M = Co, Ni) [15-18].

2. Experimental

Powder specimens of $AgCa_2Mn_2V_3O_{12}$ and $NaPb_2Mn_2V_3O_{12}$ were prepared by solid-state chemical reactions:

$$4Ag + 8CaO + 8MnO_2 + 6V_2O_5 = 4AgCa_2Mn_2V_3O_{12} + 3O_2\uparrow, \quad (1)$$

$$Na_2CO_3 + 4PbO + 4MnO_2 + 3V_2O_3 + O_2 = 2NaPb_2Mn_2V_3O_{12} + CO_2\uparrow. \quad (2)$$

The starting materials, Ag (purity 99.99 %, melting point (mp) 1235 K), CaO (99.99 %, mp 2843 K), MnO_2 (99.9 %, decomposition point 808 K), V_2O_5 (99.9 %, mp 963 K), Na_2CO_3 (99.5 %, mp 1124

K), PbO (99 %, mp 1161 K), and V_2O_3 (99.9 %, mp 2243 K), were mixed in required amounts. Mixed powder materials were placed on an alumina boat in a muffle furnace whose temperature was elevated to 1073 K for $AgCa_2Mn_2V_3O_{12}$ and 1023 K for $NaPb_2Mn_2V_3O_{12}$ and was then held for 12 h in the ambient atmosphere. The resultant specimens were reground and pressed to rectangular bars at a pressure of 0.2 GPa. The same temperature program sequences were repeated once again, respectively.

XRD data were taken with Cu Kα radiation at room temperature on a Bragg-Brentano-type powder diffractometer equipped with a curved graphite monochrometer (graphite with a curvature radius of 224 mm). The radius of the goniometer was 185 mm. The open angle of the divergence and scattering slits were both 0.5 °, and the widths of the receiving slit and the monochrometer-receiving slit were 0.15 mm and 0.6 mm, respectively. The specimen crushed sufficiently was charged into a flat glass holder. The XRD data were measured in a 2θ range from 10 ° to 120 ° with a step interval of 0.02 °. X-ray tube voltage and tube electric current were 30 kV and 100 mA for $AgCa_2Mn_2V_3O_{12}$ and 50 kV and 150 mA for $NaPb_2Mn_2V_3O_{12}$, respectively. The fixed counting times in the XRD measurements were 3 s for $AgCa_2Mn_2V_3O_{12}$ and 0.6 s for $NaPb_2Mn_2V_3O_{12}$. Details in the data collection are shown in Table 1.

The XRD data were analyzed by the Rietveld method with RIETAN-2000 [19]. We adapted the pseudo-Voigt profile function of Thompson et al. [20] made asymmetric with the procedure of Finger et al. [21], and the following reliable factors were used in the Rietveld refinements. The reliable factors of *R*-weighted pattern, R_{wp}, *R*-pattern, R_p, *R*-Bragg factor, R_B, and *R*-structure factor, R_F, are defined and expressed as [22],

$$R_{wp} = \left[\frac{\sum_i w_i \left(y_{i,\mathrm{obs}} - y_{i,\mathrm{cal}} \right)^2}{\sum_i w_i \left(y_{i,\mathrm{obs}} \right)^2} \right]^{\frac{1}{2}}, \tag{3}$$

$$R_p = \frac{\sum_i \left| y_{i,\mathrm{obs}} - y_{i,\mathrm{cal}} \right|}{\sum_i y_{i,\mathrm{obs}}}, \tag{4}$$

$$R_B = \frac{\sum_K \left| I_{K,\text{"obs"}} - I_{K,\mathrm{cal}} \right|}{\sum_K I_{K,\text{"obs"}}}, \tag{5}$$

$$R_F = \frac{\sum_K \left| \left| F_{K,\text{"obs"}} \right| - \left| F_{K,\mathrm{cal}} \right| \right|}{\sum_K \left| F_{K,\text{"obs"}} \right|}. \tag{6}$$

Here y_i is the intensity at the *i*th step, and $w_i = 1/y_{i,\mathrm{obs}}$ the statistical weight. I_K is the integrated intensity assigned to the *K*th Bragg reflection at the end of the refinement cycles, and F_K is the crystal structure factor. The subscripts obs and cal with each notation are added to the meaning of the observed value and the calculated value. For the subscripts ‘‘obs’’, I_K and F_K are not purely observed value except for the isolated reflections; thus it is estimated-observation-value obtained from programmatic allocation using the refinement parameters after the Rietveld analysis. *R*-expected, R_e, is the R_{wp} of the minimum expected statistically

$$R_e = \left[\frac{N - P}{\sum_i w_i \left(y_{i,\mathrm{obs}} \right)^2} \right]^{\frac{1}{2}}, \tag{7}$$

where *N* is the number of all the data and *P* the number of refined parameters.

Table 2
Indices, observed and calculated values of *d* spacings, and observed peak intensities (relative intensities) for $AgCa_2Mn_2V_3O_{12}$ with the lattice constant a = 12.596(2) Å

h	k	l	d_{obs} / Å	d_{cal} / Å	I_{obs}
4	0	0	3.1509	3.1488	39
4	2	0	2.8168	2.8164	100
3	3	2	2.6868	2.6853	5
4	2	2	2.5715	2.5710	44
4	3	1	2.4701	2.4701	7
5	2	1	2.2996	2.2996	6
5	3	2	2.0439	2.0432	10
6	1	1		2.0432	
6	2	0	1.9919	1.9915	1
4	4	4	1.8186	1.8180	9
6	4	0	1.7478	1.7467	24
5	5	2	1.7155	1.7140	1
6	3	3		1.7140	
7	2	1		1.7140	
6	4	2	1.6834	1.6831	47
8	0	0	1.5750	1.5744	11
8	4	0	1.4086	1.4082	8
8	4	2	1.3746	1.3743	16
6	6	4	1.3433	1.3427	6
8	5	3	1.2729	1.2723	1
9	4	1		1.2723	
8	6	4	1.1699	1.1694	11
10	4	0		1.1694	
10	4	2	1.1503	1.1498	7
8	8	0	1.1137	1.1133	5
8	8	4	1.0500	1.0496	2
12	0	0		1.0496	
12	2	0	1.0355	1.0353	3
10	6	4	1.0219	1.0216	7
12	2	2		1.0216	
12	4	4	0.9497	0.9494	2
10	8	4	0.9384	0.9388	5
12	6	0		0.9388	
12	6	2	0.9288	0.9285	2
8	8	8	0.9092	0.9090	1

Table 3
Indices, observed and calculated values of *d* spacings, and observed peak intensities (relative intensities) for $NaPb_2Mn_2V_3O_{12}$ with the lattice constant a = 12.876(2) Å

h	k	l	d_{obs} / Å	d_{cal} / Å	I_{obs}
2	1	1	5.2605	5.2587	14
2	2	0	4.5577	4.5542	7
3	2	1	3.4424	3.4426	14
4	0	0	3.2201	3.2203	23
4	2	0	2.8806	2.8803	100
3	3	2	2.7461	2.7463	1
4	2	2	2.6301	2.6293	33
4	3	1	2.5266	2.5262	2
5	2	1	2.3528	2.3518	13
4	4	0	2.2773	2.2771	2
5	3	2	2.0897	2.0896	16
6	1	1		2.0896	
6	3	1	1.8998	1.8992	2
4	4	4	1.8596	1.8592	12
6	4	0	1.7866	1.7863	22

Table 3 (*continued*)

h	*k*	*l*	d_{obs} / Å	d_{cal} / Å	I_{obs}
5	5	2	1.7534	1.7529	5
6	3	3		1.7529	
7	2	1		1.7529	
6	4	2	1.7215	1.7213	27
6	5	1	1.6359	1.6359	3
7	3	2		1.6359	
8	0	0	1.6107	1.6101	7
6	6	0	1.5181	1.5181	1
8	2	2		1.5181	
8	4	0	1.4403	1.4402	5
8	4	2	1.4056	1.4054	14
6	5	5	1.3890	1.3890	1
7	6	1		1.3890	
9	2	1		1.3890	
6	6	4	1.3732	1.3731	3
7	6	3	1.3287	1.3286	2
9	3	2		1.3286	
7	7	2	1.2755	1.2754	1
10	1	1		1.2754	
8	6	2	1.2633	1.2631	2
10	2	0		1.2631	
7	6	5	1.2282	1.2282	2
9	5	2		1.2282	
10	3	1		1.2282	
8	6	4	1.1961	1.1960	9
10	4	0		1.1960	
9	6	1	1.1858	1.1858	1
10	3	3		1.1858	
10	4	2	1.1760	1.1759	4
9	6	3	1.1478	1.1475	1
10	5	1		1.1475	
11	2	1		1.1475	
8	8	0	1.1386	1.1385	4
7	7	6	1.1129	1.1128	1
9	7	2		1.1128	
10	5	3		1.1128	
11	3	2		1.1128	
8	8	4	1.0737	1.0734	1
12	0	0		1.0734	
12	2	0	1.0589	1.0588	2
10	6	4	1.0449	1.0448	3
12	2	2		1.0448	
9	7	6	1.0000	0.9998	1
9	9	2		0.9998	
11	6	3		0.9998	
12	4	4	0.9710	0.9710	2
10	8	4	0.9602	0.9601	3
12	6	0		0.9601	
12	6	2	0.9497	0.9496	1
8	8	8	0.9299	0.9296	1
10	9	5	0.8976	0.8975	1
11	7	6		0.8975	
11	9	2		0.8975	
13	6	1		0.8975	
14	3	1		0.8975	

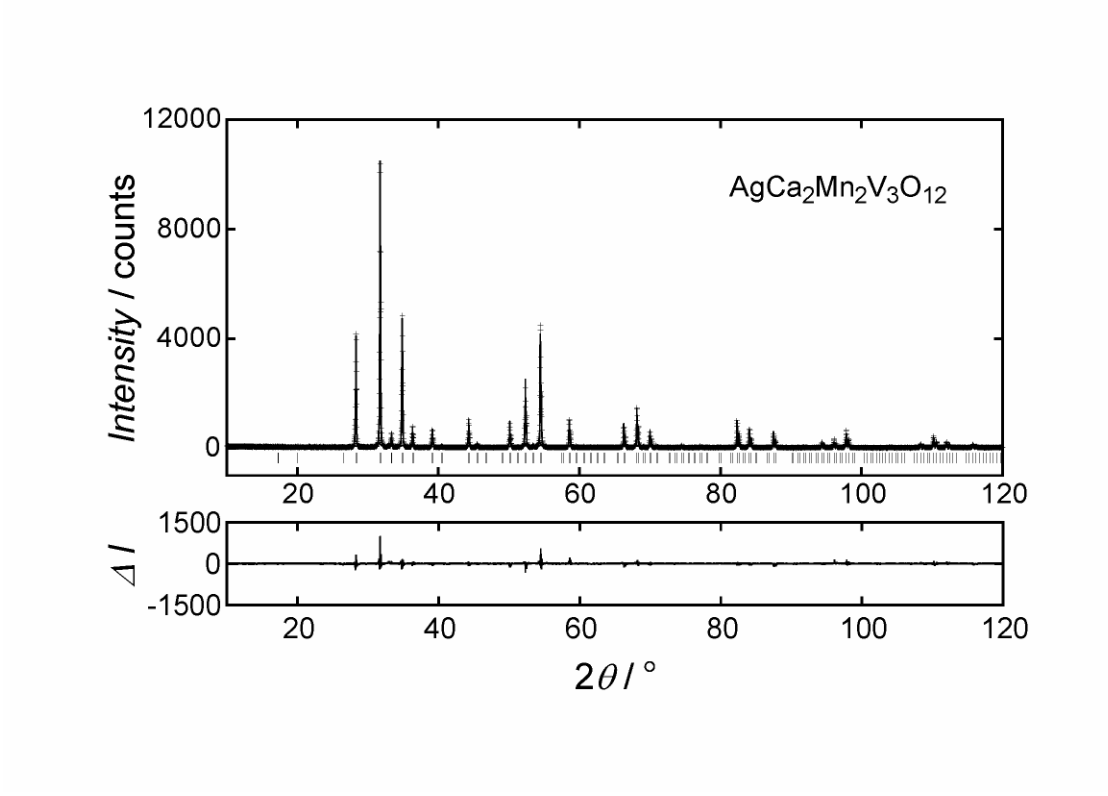

Fig. 2. Observed (+), calculated (solid line), and difference ($\Delta I = I_{obs} - I_{cal}$) patterns for the Rietveld refinement from the X-ray powder diffraction data of $AgCa_2Mn_2V_3O_{12}$. The short vertical lines below the profiles mark the peak positions of all the possible Bragg reflections.

3. Results and discussion

Extremely high-purity specimen of $AgCa_2Mn_2V_3O_{12}$ has been prepared. On the other hand, a small amount of unknown impurity has been mixed in specimen of $NaPb_2Mn_2V_3O_{12}$. This unknown impurity could not be eliminated completely, although the reaction temperature was changed from 973 K to 1073 K, and the other solid-state chemical reactions using other starting materials were attempted.

Colors of both $AgCa_2Mn_2V_3O_{12}$ and $NaPb_2Mn_2V_3O_{12}$ powder specimens were brown. In the vanadium garnets $AgCa_2M_2V_3O_{12}$ and $NaPb_2M_2V_3O_{12}$, those colors have been known to change drastically due to M^{2+} ion at the A-site in octahedron [9, 15-17]. For example, colors of the vanadium garnets are reported to be dark green for $AgCa_2Co_2V_3O_{12}$ [16], yellow for $AgCa_2Ni_2V_3O_{12}$ [16], white for $AgCa_2Mg_2V_3O_{12}$ [9], dark brown for $AgCa_2Cu_2V_3O_{12}$ [15], yellowish-white for $AgCa_2Zn_2V_3O_{12}$ [15], dark green for $NaPb_2Co_2V_3O_{12}$ [17], and yellow for $NaPb_2Ni_2V_3O_{12}$ [17].

The diffraction peaks in the XRD patterns for both vanadium garnets were indexed on the basis of cubic symmetry with space group *Ia*-3*d* except for one peak of unknown impurity in the specimen of $NaPb_2Mn_2V_3O_{12}$. The indices, the comparisons of *d* spacings between the calculated and the observed values, the observed peak intensities for $AgCa_2Mn_2V_3O_{12}$ and $NaPb_2Mn_2V_3O_{12}$ are listed in Tables 2 and 3.

The Rietveld refinements of the structures were carried out in the space group *Ia*-3*d* with Ag^+ and Ca^{2+} (or Na^+ and Pb^{2+}) at the *24c*-sites (1/8, 0, 1/4), Mn^{2+} at the *16a*-sites (0, 0, 0), V^{5+} at the *24d*-sites (3/8, 0, 1/4), and O^{2-} at the *96h*-sites (*x*, *y*, *z*). The structure parameters reported for

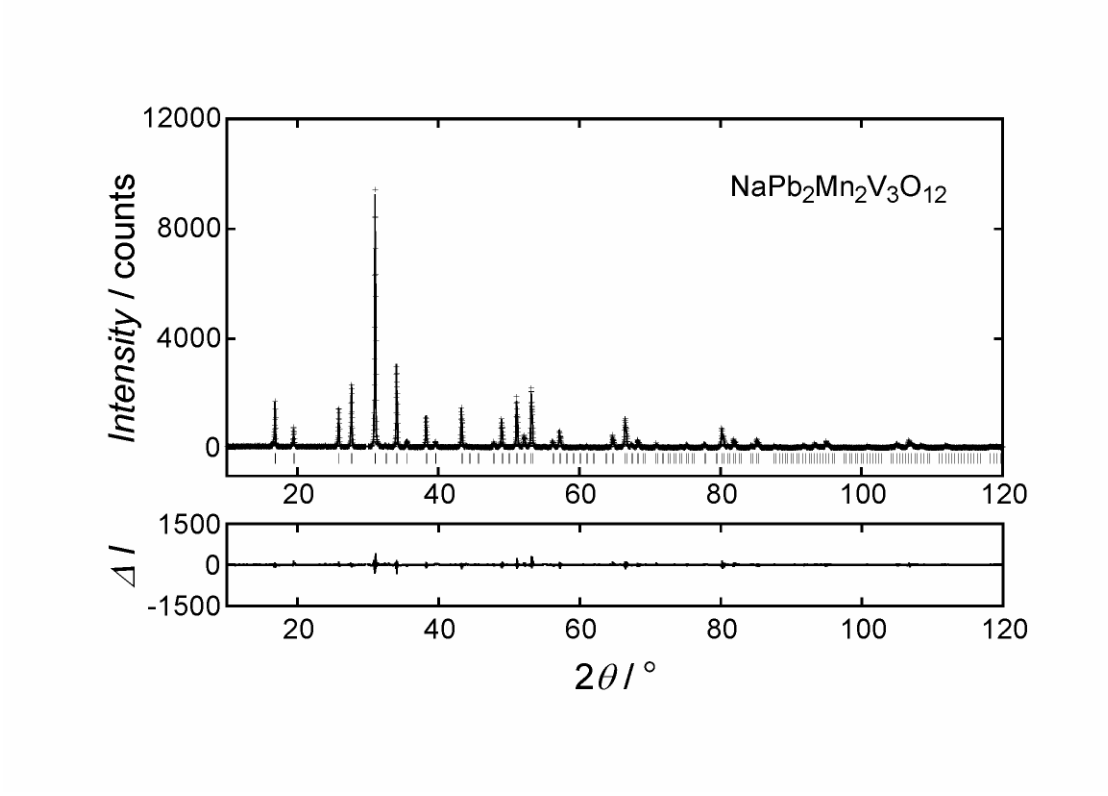

Fig. 3. Observed, calculated, and difference patterns for the Rietveld refinement from the X-ray powder diffraction data of $NaPb_2Mn_2V_3O_{12}$.

$AgCa_2M_2V_3O_{12}$ (M = Mn, Co, Ni) [10, 16] were used as a starting model. The lattice constants used as starting values were determined by the least-squares method with data of Tables 2 and 3. In the refinement of $NaPb_2Mn_2V_3O_{12}$, the 2θ range from 29.7 ° to 30.0 ° was excluded because of the existence of unknown impurity.

In Table 1, the resulting *R*-factors reached R_{wp} = 13.74 %, R_p = 9.83 %, R_B = 4.67 %, and R_F = 5.55 %, with a fit indicator of $S = R_{wp}/R_e$ = 1.33 for $AgCa_2Mn_2V_3O_{12}$ and R_{wp} = 12.18 %, R_p = 9.21 %, R_B = 3.75 %, and R_F = 3.12 %, with S = 1.33 for $NaPb_2Mn_2V_3O_{12}$. The lattice constants were a = 12.596(2) Å for $AgCa_2Mn_2V_3O_{12}$ and a = 12.876(2) Å for $NaPb_2Mn_2V_3O_{12}$. Figs. 2 and 3 show observed, calculated, and difference patterns for the Rietveld refinements from the XRD data of $AgCa_2Mn_2V_3O_{12}$ and $NaPb_2Mn_2V_3O_{12}$, and Tables 4 and 5 list the final structure parameters of these vanadium garnets.

The lattice constants reported by Ronniger et al. [9] where a = 12.596(5) Å for $AgCa_2Mn_2V_3O_{12}$ and a = 12.861(5) Å for $NaPb_2Mn_2V_3O_{12}$, and the lattice constant obtained from single-crystal data was reported to be a = 12.6084(9) Å for $AgCa_2Mn_2V_3O_{12}$ [10]. These values are in good agreement with our results.

Table 6 presents selected the interatomic distances and bond angles calculated from the XRD data of $AgCa_2Mn_2V_3O_{12}$ and $NaPb_2Mn_2V_3O_{12}$. For comparison, Table 6 also lists the interatomic distances and bond angles estimated from the single-crystal data of $AgCa_2Mn_2V_3O_{12}$ in the previous report [10]. Our new results obtained from the XRD data of $AgCa_2Mn_2V_3O_{12}$ are fairly close to those calculated from the single-crystal data. The interatomic distances were determined to be 2.150(3) Å for Mn-O and 1.698(3) Å for V-O in $AgCa_2Mn_2V_3O_{12}$, and 2.224(4) Å for Mn-O and 1.680(4) Å for V-O in $NaPb_2Mn_2V_3O_{12}$, respectively. The sum of Shannon's ionic radii [23] can be calculated at

Table 4
Structure parameters of $AgCa_2Mn_2V_3O_{12}$ determined from the X-ray powder diffraction data

Atom	Site	*g*	*n*	*x*	*y*	*z*	*U* (Å^2)
Ag	*24c*	1/3	8	1/8	0	1/4	0.0200(6)
Ca	*24c*	2/3	16	1/8	0	1/4	= *U*(Ag)
Mn	*16a*	1	16	0	0	0	0.0106(5)
V	*24d*	1	24	3/8	0	1/4	0.0049(6)
O	*96h*	1	96	-0.0406(2)	0.0506(2)	0.1579(3)	0.0206(10)

Definitions: *g*, occupation factor; *n*, number of atoms per unit cell. *U* is the isotropic atomic displacement parameter when the Debye-Waller factor is represented as $\exp(-8\pi^2 U \sin^2\theta/\lambda^2)$.

Table 5
Structure parameters of $NaPb_2Mn_2V_3O_{12}$ determined from the X-ray powder diffraction data

Atom	Site	*g*	*n*	*x*	*y*	*z*	*U* (Å^2)
Na	*24c*	1/3	8	1/8	0	1/4	0.0146(6)
Pb	*24c*	2/3	16	1/8	0	1/4	= *U*(Na)
Mn	*16a*	1	16	0	0	0	0.0123(9)
V	*24d*	1	24	3/8	0	1/4	0.0079(8)
O	*96h*	1	96	-0.0448(3)	0.0490(3)	0.1595(3)	0.016(2)

2.230 Å for Mn^{2+}-O^{2-} (CN 6, HS) and 1.735 Å for V^{5+}-O^{2-} (CN 4), which is reasonable agreement with the interatomic distances obtained by our Rietveld refinements. These results support that Mn has divalent and V has pentavalent.

To discuss oxidation state of Mn and V, the bond valence sum [24] was estimated with a computer program VICS [25]. The bond valence sum, V_i, can be considered as oxidation number of cation *i* located in the coordination polyhedron by oxygen ions *j* and is given by the empirical formula,

$$V_i = \sum_j S_{ij} = \sum_j \exp\left(\frac{l_0 - l_{ij}}{0.37}\right), \tag{8}$$

where S_{ij} is the bond valence, l_{ij} the interatomic distance, and l_0 the bond valence parameter (l_0 = 1.790 for Mn^{2+} and l_0 = 1.803 for V^{5+} [26]). The bond valence sum of Mn was calculated at 2.3 for $AgCa_2Mn_2V_3O_{12}$ and 1.9 for $NaPb_2Mn_2V_3O_{12}$, and that of V was estimated to be 5.3 for $AgCa_2Mn_2V_3O_{12}$ and 5.6 for $NaPb_2Mn_2V_3O_{12}$, respectively. Usually, the bond valence sums contain variations of about 10 % even in typical compounds, such as MnO and V_2O_5, which would be attributed to accuracy of the interatomic distances and feature of the empirical formula. Therefore, it can be considered that Mn is divalent and V is pentavalent. We are going to clarify the oxidation state of these ions from the study of their magnetism in the future works.

To investigate distortion of the MnO_6 octahedra and the VO_4 tetrahedra in both $AgCa_2Mn_2V_3O_{12}$ and $NaPb_2Mn_2V_3O_{12}$, their octahedral quadratic elongation, $\langle\lambda_{oct}\rangle$, tetrahedral quadratic elongation, $\langle\lambda_{tet}\rangle$, octahedral bond angle variance, σ_{oct}^2 , and tetrahedral bond angle variance, σ_{tet}^2, [27] were also calculated with the VICS [25]. The quadratic elongation was evaluated using the formulae,

$$\langle\lambda_{oct}\rangle = \sum_{i=1}^{6} \frac{(l_i/l)^2}{6}; \tag{9}$$

Table 6
Selected interatomic distances (Å) and bond angles (°) calculated from the X-ray powder diffraction data (this work) and the single crystal data (in Ref. [10]) of $AgCa_2Mn_2V_3O_{12}$ and $NaPb_2Mn_2V_3O_{12}$

		X-ray powder diffraction data		Single crystal data
		$AgCa_2Mn_2V_3O_{12}$	$NaPb_2Mn_2V_3O_{12}$	$AgCa_2Mn_2V_3O_{12}$
Ag/Ca – O	×4	2.471(3)		2.481(2)
Ag/Ca – $O^{(a)}$	×4	2.597(4)		2.556(2)
Na/Pb – O	×4		2.557(4)	
Na/Pb – $O^{(a)}$	×4		2.689(4)	
Mn– O	×6	2.150(3)	2.224(4)	2.161(2)
V – $O^{(b)}$	×4	1.698(3)	1.680(4)	1.722(2)
O – Ag/Ca – $O^{(c)}$	×2	64.80(10)		65.91(8)
$O^{(a)}$ – Ag/Ca – $O^{(d)}$	×2	69.15(11)		69.10(8)
O – Ag/Ca – $O^{(a)}$	×4	74.39(13)		74.64(8)
O – Ag/Ca – $O^{(e)}$	×4	73.06(10)		72.10(8)
O – Ag/Ca – $O^{(d)}$	×4	91.28(10)		92.15(8)
$O^{(a)}$ – Ag/Ca – $O^{(e)}$	×2	114.00(11)		114.11(8)
O – Ag/Ca – $O^{(f)}$	×2	118.08(10)		116.51(8)
O – Ag/Ca – $O^{(g)}$	×4	122.56(12)		122.33(8)
O – Na/Pb – $O^{(c)}$	×2		62.43(12)	
$O^{(a)}$ – Na/Pb – $O^{(d)}$	×2		67.31(13)	
O – Na/Pb – $O^{(a)}$	×4		75.84(13)	
O – Na/Pb – $O^{(e)}$	×4		73.68(13)	
O – Na/Pb – $O^{(d)}$	×4		89.91(13)	
$O^{(a)}$ – Na/Pb – $O^{(e)}$	×2		116.13(13)	
O – Na/Pb – $O^{(f)}$	×2		120.43(12)	
O – Na/Pb – $O^{(g)}$	×4		121.81(13)	
O – Mn – $O^{(h)}$	×6	89.05(12)	87.1(2)	89.95(9)
O – Mn – $O^{(a)}$	×6	90.96(12)	92.9(2)	90.05(9)
$O^{(b)}$ – V – $O^{(i)}$	×2	102.5(2)	104.1(2)	103.15(11)
$O^{(b)}$ – V – $O^{(j)}$	×4	113.1(2)	112.2(2)	112.72(11)

Symmetry codes: (a) z, x, y; (b) $1/2 + x, y, 1/2 - z$; (c) $x, -y, 1/2 - z$; (d) $1/4 - z, -1/4 + y, 1/4 + x$; (e) $1/4 - z, 1/4 - y, 1/4 - x$; (f) $1/4 - x, 1/4 - z, 1/4 - y$; (g) $z, -x, 1/2 - y$; (h) $-z, -x, -y$; (i) $1/2 + x, -y, z$; (j) $1/4 - x, -1/4 + z, 1/4 + y$.

$$\langle \lambda_{\text{tet}} \rangle = \sum_{i=1}^{4} \frac{(l_i/l)^2}{4}, \tag{10}$$

where l_i is the distance from Mn or V to ith O, and l is the center-to-vertex distance of a regular octahedron or tetrahedron with the same volume. The bond angle variance for the octahedron and the tetrahedron was calculated with,

$$\sigma_{\text{oct}}{}^2 = \sum_{i=1}^{12} \frac{(\theta_i - 90°)^2}{11}; \tag{11}$$

$$\sigma_{\text{tet}}{}^2 = \sum_{i=1}^{6} \frac{(\theta_i - 109.47°)^2}{5}, \tag{12}$$

where θ_i is the ith bond angle. From the crystal data obtained by the Rietveld refinements from the XRD data, these parameters were calculated at $\langle\lambda_{\text{oct}}\rangle = 1.00$, $\langle\lambda_{\text{tet}}\rangle = 1.01$, $\sigma_{\text{oct}}{}^2 = 1.00$ degree^2, and $\sigma_{\text{tet}}{}^2 = 29.8$ degree^2 for $AgCa_2Mn_2V_3O_{12}$ and $\langle\lambda_{\text{oct}}\rangle = 1.00$, $\langle\lambda_{\text{tet}}\rangle = 1.00$, $\sigma_{\text{oct}}{}^2 = 9.34$ degree^2, and $\sigma_{\text{tet}}{}^2 = 17.4$ degree^2 for $NaPb_2Mn_2V_3O_{12}$, respectively. The calculated values of $\langle\lambda_{\text{oct}}\rangle$ and $\langle\lambda_{\text{tet}}\rangle$ are

close to 1, and those of σ_{oct}^2 and σ_{tet}^2 are quite smaller than those of typical garnet-type compounds, e.g., σ_{oct}^2 = 45.6 degree^2 and σ_{tet}^2 = 66.8 degree^2 for $Y_3Fe_5O_{12}$ [28]. This finding shows that the MnO_6 octahedra and the VO_4 tetrahedra for both garnets are hardly distorted. For comparison, the quadratic elongation and the bond angle variance for the some garnets that same ions occupy both A- and D-sites, e.g., $R_3Fe_5O_{12}$, $R_3Al_5O_{12}$, and $R_3Ga_5O_{12}$ (R = rare earth element), were evaluated from the crystallographic data registered in the Inorganic Crystal Structure Database (ICSD) [29]. The values calculated for $AgCa_2Mn_2V_3O_{12}$ and $NaPb_2Mn_2V_3O_{12}$ were significantly lower than those for $R_3M_5O_{12}$ (M = Fe, Al, Ga). Thus, the distortions of the MnO_6 octahedra and the VO_4 tetrahedra in the vanadium garnets are significantly suppressed, comparing with those of the MO_6 octahedra and the MO_4 tetrahedra in $R_3M_5O_{12}$ (M = Fe, Al, Ga).

Finally, the lattice constants of $AgCa_2Mn_2V_3O_{12}$ and $NaPb_2Mn_2V_3O_{12}$ are compared with those obtained by the previous workers. When the combination of ions at the C-site in $\{C_3\}Mn_2V_3O_{12}$ changes from $AgCa_2$ to $NaPb_2$, the increment in the lattice constant is 0.28 Å (= 12.876(2) - 12.596(2) Å). Commeasurable increments are also found between $AgCa_2M_2V_3O_{12}$ and $NaPb_2M_2V_3O_{12}$ (M = Mg, Co, Ni, Zn), for example, 0.27 Å for M = Co and 0.26 Å for M = Ni [9, 15-17]. On the other hand, the lattice constant strongly depends on the ionic radii of the A-site cations and linearly increased with increasing of the ionic radius when the same combination of cations locates in the C-site. In addition, the Ag/Ca-O and V-O distances in $AgCa_2MV_3O_{12}$ (M = Mn, Co, Ni) are independent of size of M cation at A-site. For instance, Ag/Ca-O distances are 2.471(3) Å and 2.597(4) Å for $AgCa_2Mn_2V_3O_{12}$, 2.457(3) Å and 2.574(3) Å for $AgCa_2Co_2V_3O_{12}$, and 2.444(2) Å and 2.570(2) Å for $AgCa_2Ni_2V_3O_{12}$, respectively [16].

Acknowledgments

The authors would like to thank Mr T. Yamagishi for his helpful experimental collaboration. This research was supported by the Research Fellowships of the Japan Society for the Promotion of Science for Young Scientists (18-1415).

References

[1] K.-H. Hellwege (Ed.), Magnetic and other properties of oxides and related compounds, Landolt-Bőrnstein, New Series III/4a, Springer, Berlin, 1970, p. 315 and references therein.
[2] L. Neel, R. Pauthenet, B. Dreyfus, Prog. Low Temp. Phys. 4 (1964) 344.
[3] T. Yamagishi, J. Awaka, Y. Kawashima, M. Uemura, S. Ebisu, S. Chikazawa, S. Nagata, Philos. Mag. 85 (17) (2005) 1819.
[4] G. Menzer, Z. Kristallogr. 63 (1926) 157.
[5] R. Pauthenet, Ann. Phys. 3 (1958) 424.
[6] S. Geller, Z. Kristallogr. 125 (1967) 1.
[7] J. Awaka, T. Kurimoto, S. Nagata, Physica B 329-333 (2003) 669.
[8] J. Awaka, R. Endoh, S. Nagata, J. Phys. Chem. Solids 64 (2003) 2403.
[9] G. Ronniger, B.V. Mill, Sov. Phys. Crystallogr. (English Transl.) 18 (1973) 339.
[10] R. Rettich, Hk. Mu¨ ller-Buschbaum, Z. Naturforsch, B. Chem. Sci. 53 (3) (1998) 291.
[11] G. Ronninger, B.V. Mill, V.I. Sokolov, Kristallografiya 19 (1974) 361.
[12] K.P. Belov, B.V. Mill, G. Ronninger, V.I. Solokov, T.D. Hien, Sov. Phys. (Solid State) 12 (1970) 1393.
[13] J.M. Desvignes, P. Feldmann, H. Le Gall, J. Cryst. Growth 52 (1981) 650.
[14] A. Nakatsuka, Y. Ikuta, A. Yoshiasa, K. Iishi, Mater. Res. Bull. 39 (2004) 949.

[15] J. Awaka, R. Katagi, H. Sasaki, R. Endoh, N. Matsumoto, S. Ebisu, S. Nagata, J. Phys. Chem. Solids 62 (2001) 743.
[16] J. Awaka, N. Kijima, M. Uemura, Y. Kawashima, S. Nagata, J. Phys. Chem. Solids 66 (2005) 103.
[17] S. Nagata, T. Yamagishi, K. Awaka, J. Awaka, S. Ebisu, S. Chikazawa, J. Phys. Chem. Solids 66 (2005) 177.
[18] J. Awaka, M. Ito, T. Suzuki, S. Nagata, J. Phys. Chem. Solids 66 (2005) 851.
[19] F. Izumi, T. Ikeda, Mater. Sci. Forum 321?324 (2000) 198.
[20] P. Thompson, D.E. Cox, J.B. Hastings, J. Appl. Crystallogr. 20 (1987) 79.
[21] L.W. Finger, D.E. Cox, A.P. Jephcoat, J. Appl. Crystallogr. 27 (1994) 892.
[22] R.A. Young (Ed.), The Rietveld Method, Oxford University Press, Oxford, 1995 (Chapter 1).
[23] R.D. Shannon, Acta Crystallogr. A 32 (1976) 751.
[24] I.D. Brown, D. Altermatt, Acta Crystallogr. B 41 (1985) 244.
[25] F. Izumi, R.A. Dilanian, Recent Research Developments in Physics, Part II, Transworld Research Network, Trivandrum, 2002 (p. 699).
[26] R.E. Brese, M. O'Keeffe, Acta Crystallogr. B 47 (1991) 192.
[27] G.V. Gibbs, P.H. Ribbe, K. Robinson, Science 172 (1971) 567.
[28] A. Nakatsuka, A. Yoshiasa, S. Takeno, Acta Crystallogr. B 51 (1995) 737.
[29] Inorganic Crystal Structure Database (ICSD), Version: 2006-02, The National Institute of Standards and Technology, Fachinformationszentrum Karlsruhe, 2006.